

Amplitude Variation with Offset: Case History in Water Table and Lithological Reflection

Mahmud Mustain¹

¹*Ocean Engineering Department FTK-ITS Surabaya 60111 Indonesia*

Abstract: *The aim of this paper is to prove that the reflection seismic method available to image the water table reflection. It is to response Clement et al (1997) statement that "Seismic refraction is the only technique to image the water table". Two sets of seismic records from a difference subsequent field survey have been processed using the similar processing sequences. Both of them image a clear reflector. Edwinstow seismic record presented the water table reflector while the other is Croft set of record that presented the lithological reflector. The application of AVO analysis to CMP gathers from Edwinstow field records shows the characteristic of increase sharply amplitude with increasing angle of incidence for second critical reflection. On the other hand, the characteristic of decreasing amplitude with increasing angle of incidence for second critical reflection was presented by Croft field records. In this way the water table reflector is clearly distinguished oppositely from lithological boundaries. The results of both field survey and its interpretation are validated by equipment assessments that includes: seismograph, Promax processing system, and geophones test.*

Keywords: *geophysics, water table, shallow, seismic, reflection, AVO.*

I. Introduction

Amplitude Variation with Offset (AVO) analysis uses the phenomenon that reflection coefficients vary with source-receiver offset, which is observed on CMP pre-stack gathers (Vavrycuk & Psencik, 1998; Ruger, 1998; Lindsay & Ratcliff, 1996). This analysis has been used successfully by Ostrander (1984) to demonstrate that gas sand reflection coefficients vary with increasing offset. He also showed how to utilize the variation behavior as a direct hydrocarbon indicator on real data. AVO analysis is also used successfully as a hydrocarbon exploration tool (Santoso et. al. 1996; Sheriff & Geldart, 1995; Castagna & Backus, 1993).

Castagna & Backus (1993) described AVO, as "a seismic lithology" tool, which provides an improved model of the reflection seismogram. These properties might be directly related to lithology and fluid content. AVO analysis has also been used to identify the reservoir fluid, such as gas, water and oil by plotting the value of the P-wave velocity against Poisson's ratio (Santoso et. al. 1996, Mustain, 2009). Skidmore and Lindsay (1997) concluded that AVO analysis helps seismic imaging in deepwater environments.

The aim of the author here is to present an opportunity to use result of AVO analysis for identification of water saturated sandstone (water table in near surface) to be compared to the solid reflection. The water table should theoretically produce a clear AVO response, which very different from a lithological boundary. Therefore, we can use this manner to identify the water table by shallow seismic method as hydrological reflection. The method is to use the result of AVO analysis from the data over the land in order to image water table reflection, and to collect data for solid reflection. Next, we will show the observed AVO anomalies for both reflections, then there where should be confirmed by recorded calibration system and processing calibration system. Finally, there were would be established with the AVO analysis curves.

II. Reflection Coefficient

Referring to the simple form of Zoeppritz's (1919) equation about energy absorption that can be expressed in term of the change of amplitude for normal incidence (assuming up to 15°); we need to expand further the general case where the angle of incidence exceeds 15° . Consequently, the equations for the coefficient of reflection and transmission (as a solution of the wave equations) become more complicated. This includes the term of θ (the angle of incidence). Tooley et al (1965) showed the variation of amplitude with angle of incidence for several sets of parameters.

Figure 1 shows the P-wave reflection coefficient for various P-wave velocity ratios (v_2/v_1). The critical angle varies as the variation of P-wave velocity ratio, and gives this figure its complex appearance. When there were no impedance contrast or the velocity ratio is unity, then the reflected energy is zero (no curve for this case). The two peaks for $v_2/v_1 > 1$ occur at the critical angle for P- and S-waves, respectively (Sheriff and Geldart, 1995). In the special situation where one medium is a fluid and the other is a solid, the large amounts of S-wave energy are generated in the solid medium at large angles of incidence by P-wave incident from either medium (Tooley et al, 1965).

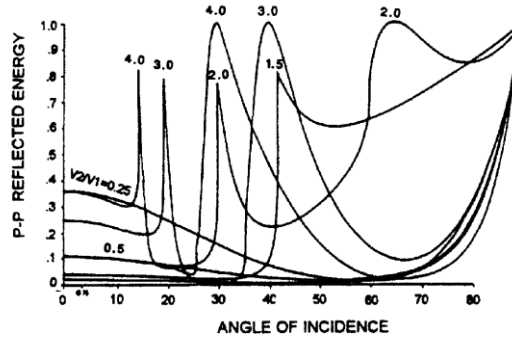


Figure 1 The effect on the P-wave reflected compression energy of varying the compression velocity ratio (V_2/V_1 or α_2/α_1) (source Sheriff and Geldart, 1995)

Aki and Richard (1980) derived the solutions to the equations for the reflected and transmitted P-wave, which is frequently used to find the amplitude variation with offset (AVO). The solution is:

$$R_p \approx \frac{1}{2} \left[1 - 4 \left(\frac{\beta^2}{\alpha^2} \sin^2 \theta \right) \frac{\Delta \rho}{\rho} + \frac{1}{2} \sec^2 \theta \left(\frac{\Delta \alpha}{\alpha} \right) - 4 \left(\frac{\beta^2}{\alpha^2} \right) \sin^2 \theta \left(\frac{\Delta \beta}{\beta} \right) \right] \quad 1$$

$$T_p \approx 1 - \frac{1}{2} \left(\frac{\Delta \rho}{\rho} \right) + \left(\frac{1}{2} \sec^2 \theta - 1 \right) \left(\frac{\Delta \alpha}{\alpha} \right) \quad 2$$

Shuey (1985) made a simplification of these equations by changing β and $\Delta \beta$ with σ and $\Delta \sigma$ with;

$$\frac{\Delta \beta}{\beta} = \frac{\Delta \alpha}{\alpha} + 0.5 \Delta \sigma \left(\frac{1}{1-\sigma} - \frac{2}{1-2\sigma} \right), \quad \beta^2 = \alpha^2 \frac{1-2\sigma}{2(1-\sigma)}$$

$$\Delta \alpha = \alpha_2 - \alpha_1 \text{ and } \alpha = (\alpha_2 + \alpha_1)/2, \quad \Delta \beta = \beta_2 - \beta_1 \text{ and } \beta = (\beta_2 + \beta_1)/2$$

$$\Delta \rho = \rho_2 - \rho_1 \text{ and } \rho = (\rho_2 + \rho_1)/2, \quad \Delta \sigma = \sigma_2 - \sigma_1 \text{ and } \sigma = (\sigma_2 + \sigma_1)/2$$

$$\theta = (\theta_2 + \theta_1)/2 \text{ with } \frac{\sin \theta_1}{\alpha_1} = \frac{\sin \theta_2}{\alpha_2}$$

Then with further modification derived by him, the relation becomes:

$$R_p \approx R_0 (1 + P \sin^2 \theta + Q (\tan^2 - \sin^2 \theta)) \quad 3$$

$$\text{Where: } R_0 = \frac{1}{2} \left(\frac{\Delta \alpha}{\alpha} + \frac{\Delta \rho}{\rho} \right), \quad P = \left[Q - \frac{2(1+Q)(1-2\sigma)}{1-\sigma} \right] + \frac{\Delta \sigma}{R_0(1-\sigma)^2}$$

$$Q = \frac{\Delta \alpha / \alpha}{\frac{\Delta \alpha}{\alpha} + \frac{\Delta \rho}{\rho}} = \frac{1}{1 + \frac{\Delta \rho / \rho}{\Delta \alpha / \alpha}}$$

R_0 is the reflection coefficient for normal incident

The simplification uses an assumption that Poisson's ratio is the elastic property most directly related to the angular dependence of reflection coefficient (Shuey, 1985). This also made a further modification to separate out the factor R_0 as the amplitude at normal incidence. It is easy to see that R_0 is an appropriate reference for $\theta \approx 0$. For intermediate angles ($0 < \theta < 30$ degree) or second critical angle, the reflection amplitude is connected to the parameter P which is the sum of the two terms. The real component of that parameter is in the ratio $\Delta \sigma / R_0$.

In the next following years, Hilterman (unpublished and private communication reported by Sheriff and Geldart, 1995) wrote the form of:

$$R_p \approx R_0 \left[1 - 4 \left(\frac{\beta^2}{\alpha^2} \right) \sin^2 \theta \right] + \frac{\Delta \sigma}{(1-\sigma)^2} \sin^2 \theta + R_0 \left(\frac{\Delta \alpha}{2\alpha} \right) \left[\tan^2 \theta - 4 \left(\frac{\beta^2}{\alpha^2} \right) \sin^2 \theta \right] \quad 3.a$$

He made a further approximation for intermediate angles that neglects the third term (dominated by velocity dependence). For a half space medium this is given by Al-Ghamdi et al (1998):

$$R_p \approx R_0 \cos^2 \theta + 2.25 \Delta \rho \sin^2 \theta \quad 4$$

The next extension for these conceptions is the author will make critical analysis for intermediate angle. This is specially to distinguish the water table reflection from the lithological reflection as normally stratigraphical reflection in near surface. The simplification of Hilterman (in Sheriff and Geldart, 1995) to neglect the third term due to the dominated of velocity dependency is to be back. The reason is the velocity dependency can not be neglected due to

significance value of difference velocity of saturated water sandstone and unsaturated sandstone. Therefore the formulation after Al-Ghamdi et al (1998) is given:

$$R_p = R_0 \left[\cos^2 \theta + \frac{\Delta\alpha}{2\alpha} (\tan^2 \theta - \sin^2 \theta) \right] + 2.25 \Delta\rho \sin^2 \theta \quad 5$$

III. Numerical Implementation Model

Clearly the mathematical AVO model is different from the physical model. The physical model (figure 1) shows the ideal natural condition. The model can treat the signal continuously from normal incidence to wide angle (90°) in the laboratory's experimentation, and the 1st and 2nd critical angle should appear. However, the mathematical model cannot cover the complete formulation as a complex form (Koefoed, 1962). Only the real part can be used in practice and this has to be approximated for three zones: normal incidence, intermediate angle, and wide angle (Shuey 1985, Ostrander, 1984). In this case history (study) we only used intermediate angles 24° was the first critical angle and 35° was the widest data provided. Consequently, we cannot see any critical angle reflection after 35°.

The AVO curve for three different approximation formulae (Aki & Richards 1980; Shuey 1985; and Hilterman by Sheriff & Geldart 1995) were have been calculated for a water table reflection in a pure sandstone with 30% porosity. Figure 2 shows the calculated curves of different formulae for intermediate angles. Each formula has different specifications. Aki & Richards (1980) reported that their formula is only valid when; $\Delta\alpha/\alpha$, $\Delta\beta/\beta$, and $\Delta\rho/\rho$ are small and $\theta < 10^\circ$ if $\alpha_1 < \alpha_2$. Although the amplitudes are not the same for normal incidence, the lithology and water table curves have opposite trends (decrease and increase respectively curve of A&R-lit and A&R-wt). This is because Aki & Richards formula does not separate the R_0 factor while the other formulae do.

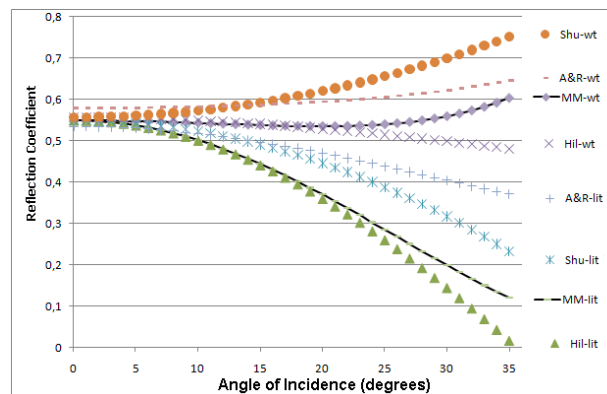


Figure 2 The curve of AVO for water table in typical sandstone of 30 % porosity using; 1. Hilterman formula (eq. 4) as Hil-lit and Hil-wt, 2. Shuey (eq. 3) as Shu-lit and Shu-wt, 3. Aki & Richards (eq.1&2) as A&R-lit and AR-wt, and 4. Mustain Modification formula after Al-Ghamdi (eq 5) as MM-lit and MM-wt. $R_c=0.2$, lithology velocity $\alpha_1 = 840$; $\beta_1 = 0.5 \alpha_1$; $\alpha_2=2050$; $\beta_2=0.5\alpha_2$, Water table velocity $\alpha_1 = 840$; $\beta_1 = 0.5\alpha_1$; $\alpha_2=2050$; $\beta_2 = 0.5\alpha_1$

The implementation of the Shuey formula in this case study gives the value of the dimensionless parameter of $P = -0.1$ for lithology and $P = 0.9$ for water table. The curve of Shu-wt shows that the relative amplitude increases sharply as the water table (figure 2). On the other hand, for the same effect the curve of Shu-lit decreases. This is important evidence that this formula can indicate water table anomalies. The middle term of the Shuey formula (eq. 3) controls R_p , and the last term is always positive. This implementation of the Shuey formula produces a value $R_0 = 0.56$, very close to the coefficient reflection value from R_c versus porosity curve of water saturated sandstone that gives $R_0 = 0.53$ for 33% porosity. There is a reasonable agreement between the ideal calculation of the R_c versus porosity curve and the mathematical implementation of Shuey formulae.

The Hilterman (by Sheriff & Geldart 1995) approximation also can be used to this application. For the Lithology case, the Hil-lit curve has a same negative trend to the Shu-lit curve at most angles. However, for the Water Table gives rather a different result, Hil-wt curve shows negative trend (amplitude decreases with increasing of angle of incidence) while the Shu-wt is positive (amplitude increases with increasing of angle of incidence). This is because the Shuey approximation is more relevant for a case using intermediate angles. On the other hand, Hilterman uses the approach of half space of velocity ($V_2 = 2V_1$). Both Shuey and Hilterman approximations clearly prove that the lithological boundary and water table (as hydrological boundary) have opposite trends, decreasing and increasing respectively. This also indicates that $R_p = R_0$ for $\theta \approx 0$.

One importance point in this paper is the proposed formula of equation 5 to be made on the implementation as the alternative formula in order to the water table reflection. These cases are also would be fixed as the mathematical forms for water table reflection (MM-wt) and lithological reflection (MM-lit). The most different result gives us very interested interpretation, the curve is MM-wt on the range of 25° to 35°. The curve sharply increases on that range i.e. the range of the second critical or intermediate angle. This is very good evidence that the amplitude go up on this offset for water table reflection.

1 Observed AVO of Edwinstowe Section for Water Table Reflection

Part of Edwinstowe (25 km north of Nottingham, UK) common offset gathers has been chosen for AVO analysis (Mustain, 2002). Common offset gather for this case study is have been chosen, figure 3. A possible reason is the homogeneous nature of the subsurface geology. There were some processes required to reduce factors that affect the seismic amplitude, especially factors with offset dependence.

Referring to the physical model (figure 1) as a representation of a complex formulation for normal or natural condition, it is representative of the Edwinstowe condition that has a compression velocity ratio V_2/V_1 of 2.5. The intermediate angle range is from 24° (as the first critical) to 50°. The observational data is only available for the range of angles from 24° to 35°. Within this more limited range, the reflected energy decreases sharply with increasing angle of incidence. The model curves in figure 1 are computed for boundaries with a lithological contrast, where the partition of energy is mainly controlled by the properties of the matrix of the rock and not its fluid content.



Figure 3 a part of Edwinstowe record as the result of 15 Common Offset stack (source Mustain 2002)

Figure 4 illustrates the result of AVO record from figure 3 and mathematical model of both lithological and hydrological boundaries (reflections). The stack-wt (figure 4) is the result of stacking using common offset by Promax, while the Manu-wt is the result of manual averaging from 15 shot records. Both plotted stack and plotted manual have the expected trends i.e. increasing amplitude with increasing offset. These curves increase sharply from 28.1° until 32°. This increase is good evidence that the reflector is a hydrological boundary (water table), oppositely if the curve decreased with increasing offset then it would be a lithological boundary (figure 4, solid and dashed line are the mathematical model for water table and lithological boundary respectively).

The error bars, from standard deviation of the averaging record (from manual picking) is 17.5 % with a maximum deviation of 29 %. Statistically, this distribution record is normal, as indicated by the maximum deviation among the data being greater than its standard deviation. The instrumentation test gives a result of the seismograph channel having an average deviation of 0.3%, and all geophone tests gives average deviations of 9.7%, with processing system tests indicating deviations of less than 2% (1.20 %, 0.02 %, and 0.81 % for error of: f-k filter, top mute, and band pass filter respectively). Thus it is reasonable to conclude that the variation of amplitude is statistically caused by variation in offset, not the instrumentation. To confirm this, it will be proved by AVO analysis of a known lithological boundary, which shows that the amplitude decreases with offset.

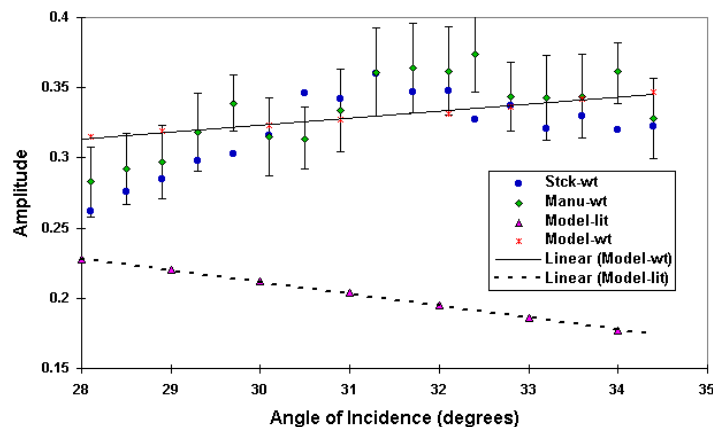


Figure 4 AVO analysis of Edwinstowe record as average (promax stacking as Stack-wt and manual averaging as Manu-wt) of 15 common offset gathers with average deviation of 17.5 % as error bars, comparing to the mathematical model using Shuey formula as lithological and water table boundary (Model-lit and Model-wt)

2 Observed AVO of Croft Record for Lithological Reflection

The main purpose of this section is to apply AVO analysis to a reflection from a lithological boundary. This boundary will prove that the amplitude decreases with increasing offset in the intermediate angle (between P and S critical angles). Previously, we have proven that the amplitude increased with increased offset for water table reflection as hydrological boundary.

This investigation needs data with appropriate post critical reflection, which we can analyze the trend of amplitude Vs offset for the same purpose as Edwinstowe survey. Croft records that had been taken one year before Edwinstowe are appropriate data for this purpose. This has a simple geophysical target, of a flat lying reflector. The records have a maximum offset of 136m, which is adequate when using AVO analysis for a depth of target of about 100 m. This gives us a chance to analyze ranges beyond the critical angle.

The field area is located near Croft Quarry (SP 523 956) South Leicester, UK. The site is a small field west of Coventry road, beside the quarry entrance. Figure 5 shows the plan of the shot line of seismic survey. It is a covering of 100-200m of bedded sediment (Mercian Mudstones underlying Sherwood Sandstone) unconformable overlying a granitic intrusion. Mudstones are flat lying, and no ray paths we considered to have entered the granite. This is geologically similar to the Edwinstowe location analysed for water table reflection. The primary interest of this site is to determine the depth of Mesozoic/Palaeozoic cover over diorite rock east of Croft Quarry.

The processing sequence is similar to the processing for both the synthetic and the Edwinstowe records. Figure 6 shows the final stack. The figure shows that there are three simple layers with first and second boundary at around 100 and 150m respectively, meaning the basement starts in the third layer. This also indicates that the zone below this boundary has no significant layering. This may be due to the very limited length of record.

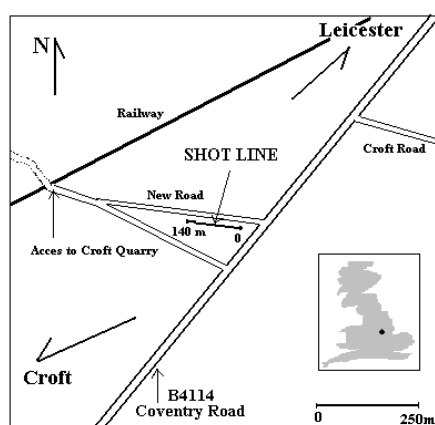


Figure 5 The plan location of shot line of seismic survey

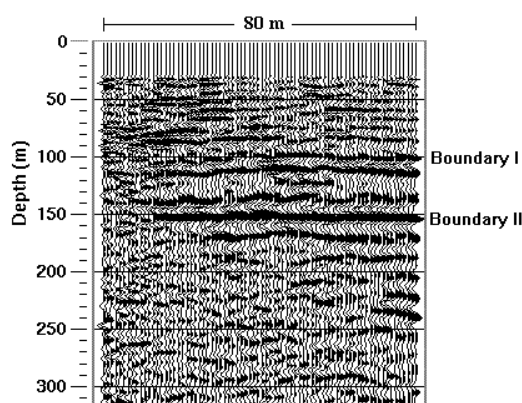


Figure 6 The final stack of Croft record

The prominent reflector at the first boundary at 100 m is interpreted as a contrast in velocity from 1900m/s to 4150m/s. The reflector is very difficult to interpret as the depth of Mesozoic/Palaeozoic (Mercian Mudstone) cover over diuretic rock East of Croft Quarry, is between 100-200m thick. The velocity of the second layer is too high for diuretic rock. Regarding to geologists within the department (Geology in Leicester University, UK) and the consensus of opinion, if there is a high velocity in the Croft data then it is probably (1) Stocking ford shale's (Cambrian) or (2) Gypsum in the Mercian Mudstone (but not halite).

According to the amplitude record for AVO analysis, CMP gather is the best section for analysis (Ostander 1984, Sheriff and Geldart 1995). CMP gathers were also used in this observation. There are 22 CMP (numbers 50 to 72) gathers, which include the maximum offset that we have (136m).

The P-wave critical angle in this AVO analysis is calculated from the estimation of critical offset (can be seen in the pick of amplitude curve in figure 7). This is in distance between 108 to 110 m and 100m of reflector depth. From this calculation, the critical angle is about 28°. This can be accepted by using the velocity contrast in the reflector, for 1900 to 4150 m/s that give the critical angle of 27°. The different of 1° is in the range of error bar of V_{rms} that less than 7 %.

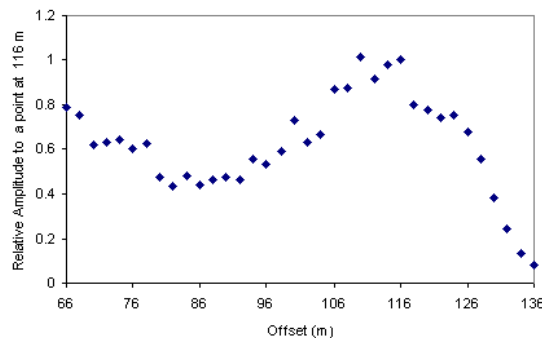


Figure 7 the AVO observation from the Croft record shows the P-wave critical angle at about 110 m

This evidence proves that the sub-critical angle has an amplitude variation with offset by providing the curve with different ways of shooting that have similar curves. Figure 8 shows the curve of AveSR2&3 that has an amplitude variation with offset from East-to-West shot. The opposite direction (West-to-East shot) is illustrated by the curve of SR48 and SR49. All the curves have similar trends, going down from 66m, having a minimum of 80-90m, and then rising to the critical angle 110-116m. All of these curves have average standard deviations of 0.57 after reducing 76 % from 3.3 (also in standard deviation) by normalization using the factor of the square root of the energy and by a random filter of 7 % wing smoothing data. This remaining error (standard deviation of 0.57) is reasonable due to the variation in geophones we have tested.

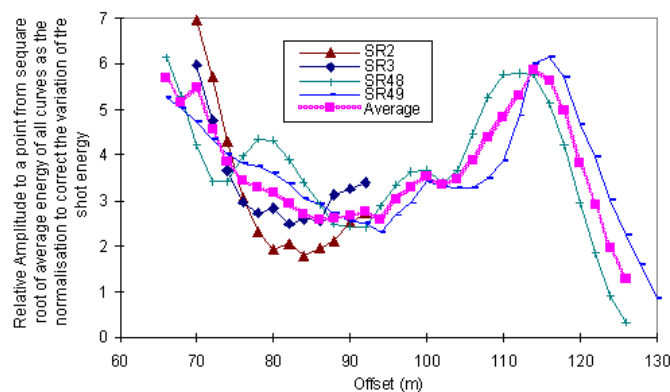


Figure 8 the curves of East-to-West shot (AveSR2&3) and the energy spectrum of most West-to East shot (SR48&49), both of them have deviation about 9 %

The AVO observation was carried out after the sequence of AVO processing similar to that of the Edwinstowe records. Figure 9 shows four AVO curves from both real data and mathematical models. Each involves lithological boundaries and water tables as hydrological boundaries from Croft and Edwinstowe records respectively. Each point has been normalized to the point at position of 28.2°. This normalization will reduce the effect of the variation of the energy source, instrument gain, and the lateral variation of layer. Data lithology (Data-lit) has been taken from a super gather as a stack of 22 CMP gathers. Although individual CMP gathers do not give any trend, the stack from the CMP gather still gives representative curves that have decreasing amplitude with increasing offset. This evidence proves that the lithological boundary produces a negative AVO gradient.

The straight lines are the linear of four curves. We can see that both data and models of linear curves are joined at the point of 28.2 ° but in different places, (the model is exactly at 1 and the data is at about 1.07). This is because the linear of model point is from of the data that has very a small variation, while the data point has a much wider variation. The slope of both Data-lit and Data-wt are also higher than both Model-lit and

Model-wt, because the real data has more complex parameters than the model. The most important consideration is that the application of AVO analysis gives sufficient evidence that amplitude increases with increasing offset for water table reflection as a hydrological boundary for both the model and real data. Conversely, the amplitude decreases with increasing offset for sub-bedding reflection as a lithological boundary for both model and real data.

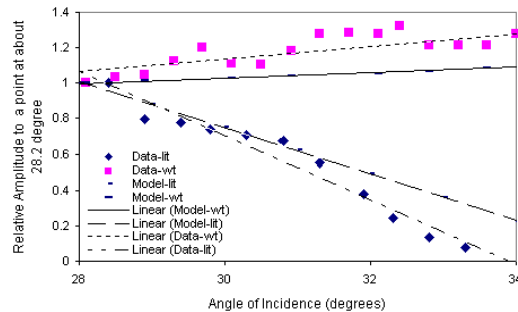


Figure 9 AVO analysis from mathematics model and observed data (Water table from Edwinstowe and lithology from Croft record) after converted to angle of Incidence (degrees)

IV. Discussion

There are four points that we set this work in geophysical context.

1. We have shown that data can be collected with high enough quality to allow imaging shallow water table reflection.
2. We have further shown that AVO analysis of this data process a water table as liquid-surface reflector.
3. This is important as a continuing progressive in development of shallow reflection method, little additional field effort and additional processing time.
4. We note that there are two still problems;
 - a. Reducing coherent noise, to allow examination of sub-critical response.
 - b. Demonstrating separation of AVO response of closely spaced lithological and hydrological boundary.

V. Conclusion

The Croft data has specifications that are appropriate for application to the AVO analysis of lithological boundaries. The velocity structure of three simple layers is interpreted as geophysical interpretation, even if there is a high velocity (second layer) in the Croft data that is probably (1) Stocking ford shale's (Cambrian) or (2) Gypsum in the Mercian Mudstone (but not halite). Edwinstow seismic record presented the water table reflector as hydrological boundary (Mustain, 2009, Mustain, 2010) was appropriate to be used to the comparison analysis .

The AVO curve shown in figure 9 establishes that the offset is also for post critical angles, which the critical angle at about 110m offset. As mentioned before, (Edwinstowe data) the focus of our AVO analysis is the post critical angle. Therefore, this figure is good evidence for both lithological and hydrological boundaries, and for mathematical models and observed data.

Acknowledgement

The authors wish to thank to the Department of high education of Indonesian Government to finance the research in Leicester University, UK.

References

- [1] Aki, K. And P.G. Richards, Quantitative Seismology: Theory and Method, San Fransisco: H.W. Freeman, 1980. (Book).
- [2] Al-Ghamdi, M.A. Rasheed A. Jaradet and Rene O. Thonsen, Predicting Up normal Reservoir Pressures using Offset Dependent Reflectivity: Theoretical Consideration, Energy Exploration and Exploitation, 1998, 16(4), 355-372. (Proceeding).
- [3] Castagna, J.P. and M.M. Backus, Offset-dependent Reflectivity: Theory and Practice of AVO Analysis, Soc. Exp. Geophysics, 1993, 3-36. (Journal).
- [4] Clement, W.P, S. Cardimona, A.L. Andres and K.K. Cade, Site Characterization at the Groundwater Remediation Field Laboratory, 1997, The Leading Edge, The society of Exploration Geophysicists, Oklahoma, 16(11), 1617-1621.
- [5] Koefoed, O., Reflection and Transmission Coefficient for Plane Longitudinal Incident Wave, Geophysical prospecting, 1962, 10, 304-351. (Journal)
- [6] Lindsay, R.O. and Ratcliff D., Amplitude Changes with Offset Evident in Subsalt Data, Oil & Gas Journal, 1996 Oct, 28, 51-60. (Journal)
- [7] Mustain, M., 2002. Confirmation of AVO Analysis to Shallow Seismic Reflection Method for Identification of the Water Table, In Proceeding of Martec2002, The Third Regional Conference on Marine Technology for The System Operational Success in the Marine Environment, July 2002, Institute Technology of Sepuluh November, Surabaya-Indonesia. p. 98-106. (Proceeding).
- [8] Mustain, M., 2009. Amplitude Vs Offset (AVO) and Poisson's Ratio Analysis to Shallow Seismic Reflection Method for Identification of the Water Table, In Seminar Nasional Pasca Sarjana V ITS 2005. DII:1-8. (Proceeding).

- [9] Ostrander, W.J., Plan-wave Reflection Coefficients for Gas Sands at Non-normal Angle of Incidence, *Geophysics*, 1984 Oct, 49(10), 1637-1648. (Journal)
- [10] Ruger, A., Variation of P-wave Reflectivity with Offset and Azimuth in Anisotropic Media, *Geophysics*, 1998 May-June, 63(3), 935-947.
- [11] Santoso, D., S. Alam, L. Hendrajaya, Alfian S., Munadi and Purwoko, Reservoir Fluid Identification and Elastic Modulus Determination using AVO, *Applied Geophysics*, 1996, 35, 159-165.
- [12] Sheriff, R.E. and Geldart, L.P, *Exploration Seismology*, 2nd Edition, Cambridge University Press, 1995 (Book).
- [13] Shuey, R.T., Simplification of the Zoeppritz Equation, *Geophysics*, 1985 Apr, 50(4), 609-614. (Journal)
- [14] Skidmore, C. and R.O. Lindsay, AVO Help Seismic Imaging in Deep Water Environments, *Oil & Gas Journal*, 1997 Nov, 3, 55-60. (Journal)
- [15] Tooley, R.D., T.W. Spencer, and H.F. Sagoci, Reflection and Transmission of Plane Compression Wave, *Geophysics*, 1965, 30(4), 552-570. (Journal)
- [16] Vavrycuk, V. and Psencik I., PP-wave Reflection Coefficients in Weakly Anisotropic Elastic Media, *Geophysics*, 1998 Nov-Dec, 63(6), 2129-2141. (Journal)
- [17] Zoeppritz, K., 1919, Erdbeben Welen VIII B, on the Reflection and Propagation of Seismic Wave, *Cottinger Nachrichten*, I, 66-84. (Journal).